

EEG Detection and Prediction of Freezing of Gait in Parkinson's Disease Based on Spatiotemporal Coherent Modes

Jun Li, Yuzhu Guo

Abstract— Objective: Freezing of gait (FOG) in the Parkinson's disease has a complex mechanism and is closely related brain activities. Timely prediction of FOG is crucial to fall prevention and injury avoidance. Traditional electroencephalogram (EEG) processing methods extract time, spatial, frequency, or phase information separately and use them or their combinations, which fragment the connections among these heterogeneous features and cannot completely characterize the whole brain dynamics during the occurrence of FOG. **Methods:** In this study, dynamic spatiotemporal coherent modes during the FOG were studied and the associated FOG detection and prediction were proposed. For capturing the changes of the brain, dynamic mode decomposition (DMD) method was applied. Dynamic changes of the spatiotemporal modes in both amplitude and phase of motor-related frequency bands were analyzed and an analytic common spatial patterns (ACSP) was used as a spatial filter to extract the essential differences among the normal, freezing and transitional gaits. **Results:** The proposed method was verified in practical clinical data. Results showed that in the detection task, the DMD-ACSP achieved an accuracy of $89.1 \pm 3.6\%$ and sensitivity of $83.5 \pm 4.3\%$, respectively. In the prediction task, an $83.5 \pm 3.2\%$ accuracy and $86.7 \pm 7.8\%$ sensitivity were achieved. **Conclusion:** Comparative studies showed that the DMD-ACSP method significantly improves the FOG detection and prediction performance. Moreover, the DMD-ACSP reveals the spatial patterns of dynamic brain functional connectivity which best discriminate the different gaits. **Significance:** The spatiotemporal coherent modes may provide useful indication for transcranial magnetic stimulation neuromodulation in medical practices.

Index Terms—Freezing of gait, EEG, brain mode decomposition, dynamic mode decomposition, dynamic functional connectivity, analytic common spatial patterns

I. INTRODUCTION

PARKINSON'S disease (PD) is a chronic neurodegenerative disease. The major motor symptoms include rest tremor, myotonia, and bradykinesia [1]. Freezing of gait (FOG) is the most common and disabling pathological gait in advanced Parkinson's disease and is manifested as transient

This work was supported in part by the Beijing Natural Science Foundation of China under Grant 4202040 and in part by the National Natural Science Foundation of China under Grant 61876015.

Jun Li is with the College of Electronic Science and Engineering, Jilin University, Changchun, China.

Yuzhu Guo is with the Department of Automation Science and Electrical Engineering, Beihang University, Beijing, China (e-mail: yuzhuguo@buaa.edu.cn).

block of movement [2]. Patients begin to hesitate, cannot walk, or feel like their feet are “glued” to the floor or sucked by the floor when walking. Freezing of gait often presents asymmetric episodes [3], [4]. FOG has been thought as a sign of Parkinson's disease entering the intermediate and advanced stages. FOG often lead to frequent falls, injuries, and even severe fractures and seriously threatening the quality of life of patients and increase healthcare burden [5].

Prompt detection and prediction of FOG are of great significance for fall prevention and injury avoidance. FOG can be identified by different data patterns exhibited by multiple sensory information, such as accelerometers [6], gyroscopes [7], [8], EEG [9], skin conductance [10], camera-based action recognition [11], and so on. Compared with other physiological signals, EEG which directly reflect brain dynamic activities during FOG attacks is expected to obtain better prediction performance. Moreover, study on EEG can provide new insights into the mechanism of FOG [12].

Existing FOG detection based on EEG information mainly includes the following methods: time-frequency analysis [13]–[16], phase analysis [13], connectivity methods [17], and so on. The time-frequency domain analysis tools include Short Time Fourier Transform (STFT), Wavelet Transform (WT), Empirical Mode Decomposition (EMD) [18] and Hilbert-Huang Transform (HHT) [19], etc. For example, Handojoseno et al. [14] proposed a FOG EEG classification algorithm based on wavelet analysis to extract the wavelet energy and wavelet energy entropy of the corresponding channel. First, a fast discrete wavelet transform was performed on the original EEG. Then, 5 common EEG frequency bands were obtained by wavelet decomposition. The wavelet energy and wavelet energy entropy features were extracted, and the patients' different synchrony was classified. The connectivity analysis method used directional transfer function to characterize the effective connection among the EEG channels and also achieved an excellent recognition performance [17].

However, existing EEG-based FOG detection techniques have the following imperfections.

- 1) Most methods using channel-by-channel extracted time-frequency features fragment the interaction among EEG channels.
- 2) Many FOG detection methods only use either the amplitude features (such as classic common spatial patterns), or phase information (such as Phase locking value, Phase lag index, and other functional connectivity methods

- based on phase synchronization) ignoring the co-action of magnitudes and phases of different functional regions.
- 3) Many methods use selected locally distributed channels in frontal, parietal or occipital lobes based on prior knowledge. These local information based method cannot fully reveal the the whole brain dynamics during FOG attacks.

Dynamic Mode Decomposition (DMD), which has been widely used in fluid dynamics research, is capable of discovering the dynamics, underlying in the spatiotemporal coherent structure of high-dimensional complex fluid phenomena using a data-driven approach, provides a new path to studying the brain dynamics [20], [21]. DMD methods have been applied to ECoG-based neural activity decoding [22]. By extracting the DMD modes contained in neural activity (described in the form of a complex matrix), modes which are composed of a combination of amplitude, phase, and frequency information can be obtained, thereby obtaining spatiotemporal coherent modes of neural activity. The research on EEG modes extraction methods based on DMD is still very limited [23].

Spatial filtering is another widely used method in EEG analysis. Classic Common Spatial Pattern (CSP) method which extracts the spatial distribution components of each type of variance information from multi-channel EEG data, is the mostly common used method [24]. However, the second order moment information used in CSP discards the phase information in EEG. Camilleri proposed an Analytic Common Spatial Pattern (ACSP) by performing discrete Hilbert transform on original EEG signal to convert EEG into analytic complex signals. Using the idea of CSP, a complex-valued spatial filter is obtained and used for spatial filtering [25]. The ACSP method extends the CSP to the complex signals and preserves both magnitude and phase information.

In this paper, combining the DMD and ACSP methods, a DMD-ACSP method is proposed to study the dynamic changes of the EEG spatiotemporal coherent modes during FOG. The DMD modes and common space pattern reveals the dynamic functional connectivity among different regions of the brain in the interested rhythms. The CSP feature of DMD modes is used to detect and predict the onset of FOG. The contributions of this study are summarized as follows.

- 1) A new DMD-ACSP model is proposed to study the whole brain dynamic functional connectivity. Using the DMD method, the EEG modes in brain dynamics are characterized in the form of DMD modes. Subsequently, the DMD mode matrix is spatially filtered with ACSP, so that mode features containing time domain, frequency domain, spatial domain, and phase information are obtained.
- 2) Through the sliding window method, the dynamic changes between normal gait, transitional gait, and freezing of gait are analyzed. The relationship between phase and amplitude between channels is observed in key frequency bands, and the main function of different gait is established connection change feature.
- 3) Cross-individual FOG detection and prediction are performed on practical EEG data. The results show that

DMD-ACSP achieves FOG classification with satisfying accuracy and generalization performance.

II. METHODS

A. Materials

The data adopted the Beihang-Xuanwu multimodal freezing of gait dataset [26]. The data collection was completed in Xuanwu Hospital Affiliated to Capital Medical University (ethical approval number: 2019-014). Each subject signed a written informed consent. The data included 12 PD patients who experienced FOG in their daily lives. Their age ranged from 57 to 81 years (mean \pm standard deviation: 69.1 ± 7.9), and disease duration ranged from 1 to 20 years (mean \pm standard deviation: 9.3 ± 6.8). All participants were able to walk independently during the experiment without severe vision and hearing loss, dementia, or other neurological disorders. Patients were off medication for more than 12 hours prior to the experiment to increase the likelihood of triggering FOG episodes in subsequent experiments, resulting in a more balanced dataset.

Patients completed the Freezing of Gait Questionnaires (FOG-Q) and Mini-Mental State Examination (MMSE), which is used to assess the clinical characteristics of patients with PD. Their FOG-Q scores ranged from 8 to 21 (mean \pm std: 16.2 ± 4.2). The Unified Parkinson's Disease Rating Scale assesses the severity of the disease in patients, classified as stages I to IV, with means of 10.4 ± 5.5 , 16.3 ± 10.6 , 45.0 ± 16.0 , and 2.2 ± 2.9 , respectively. The MMSE is used to measure cognitive impairment in patients, and their scores ranged from 24 to 30, indicating that all patients had no cognitive deficits. The study was ethically approved by the Ethics Committee of Xuanwu Hospital, Capital Medical University, Beijing, China (No. 2019-014), according to the declaration of Herbolski. Each participant signed an informed consent form. Following a standardized experimental paradigm that was effective in inducing FOG, each patient was asked to complete two types of tasks. In the first type of task, the patient started in a sitting position in a small room, then went straight to a narrow corridor, turned to the right in the corridor, turned around counterclockwise, went around a randomly placed obstacle, and returned to the starting chair. In the second type of task, patients were asked to make a U-turn and return to the starting chair within a limited space. Each patient was required to complete the experiment two to three times, taking approximately 10 to 35 minutes.

EEG signals were recorded using a 32-channel wireless system MOVE (BRAIN PRODUCTS, Germany). A total of 25 EEG channels were acquired for this experiment, and the specific channels measured refer to [26].

B. Data pre-processing

After annotation of the experimental video by two clinicians, normal gait was distinguished from FOG. The total duration of the experiment was approximately 222 minutes, of which freezing of gait accounted for 39.6% of the total duration of the experiment. Therefore, ten of the twelve

subjects were selected for data analysis. The ten subjects were sequentially labeled as Sub.1 to Sub.10 for differentiation.

The original EEG signal sampling frequency is 1000Hz. To align with other sensor data, the EEG signal was down-sampled to 500Hz. The EEG data were preprocessed using the EEGLAB toolbox. Independent component analysis (ICA) was used to remove ocular artifacts by referring to the mean signal of the temporal mastoid. The 50Hz noise was then filtered out with a notch filter and filtered by a low pass filter with a cutoff frequency of 62.5Hz.

The data were segmented using a sliding window method with a window length of 2 seconds and a step size of 0.25 seconds. In this project, in order to complete the detection task and the prediction task respectively, the experimental samples were divided into three categories, namely: the transitional gait period of 5 seconds before freezing, the normal gait period from the end of the freezing period to 5 seconds before the next freezing of gait period, and freezing gait period. Specifically, we labelled the window where more than 75% of the points are marked as freezing as the freezing gait period; we used the end of one freezing gait period as the starting point and the first five seconds to the next freezing gait period as the ending window , marked as the normal gait period; the rest was marked as the transitional gait phase.

C. Extraction of spatiotemporal modes with dynamic mode decomposition

EEG is a high-dimensional, nonlinear, non-stationary signal that contains rich brain activity information [27], [28]. It is extremely difficult to comprehensively describe the time, frequency, space, and phase changes in the process of brain activity, which is similar to nonlinear turbulence in fluid mechanics. DMD method is based on data-driven to reveal coherent modes of dynamic fluid processes from observational data. It is one of the commonly used tools in turbulence analysis, and it has a good characterization mode for nonlinear fluid dynamics. Inspired by the study of turbulence, we combined the DMD method with the ACSP method, and proposed the DMD-ACSP algorithm (Fig.1), which made it suitable for processing high-dimensional dynamic nonlinear EEG data to obtain its time domain, frequency domain, and spatial domain coupling dynamic characterization of the coupling between.

Suppose brain activity can be described by the following nonlinear state transition equation.

$$s_{t+1} = f(s_t). \quad (1)$$

where the subscripts denote discrete sampling times, i.e. the brain states are denoted as $s_0, s_1, \dots, s_n, \dots$. The traditional linearization method performs linear approximation in the field of equilibrium state, and studies its local linear dynamic performance based on linear system theory. However, this linearization method is only effective locally near the equilibrium point under weak nonlinear conditions. Due to the strong nonlinearity and non-stationary of brain activity, traditional linearization methods cannot construct a panorama of brain dynamic activity.

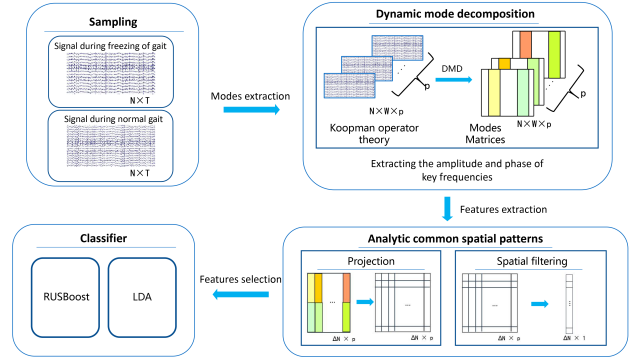


Fig. 1. Architecture diagram of the DMD-ACSP model. Upper-left: Data collection and division. Upper-right: Dynamic mode decomposition method. Lower-right: Analytic common spatial patterns. Bottom-left: Classification.

The *Koopman* operator theory provides a global linearization method based on nonlinear observation functions. *Koopman* operator, proposed by B. O. Koopman in 1931, can represent a nonlinear dynamic system of finite dimension as a linear system under the observation space of infinite dimension, thereby linearizing the system [29].

The *Koopman* operator on infinite-dimensional observation space is defined as:

$$\mathfrak{K}g(x_n) = g(x_{n+1}). \quad (2)$$

where the function $g(\cdot)$ is an observable quantity of the state of the system in an infinite-dimensional function space. The *Koopman* operator describes the linear evolution process of the value of the observable g in the observation space, that is, the value of the observable g at the initial moment is $g(x_0)$, then the value of the observable g becomes $g(x_p) = \mathfrak{K}^p g(x_0)$ after p steps of evolution.

In this paper, the dynamic activity of brain activity in the EEG observation space is studied using the EEG (and its delay) as the subspace of the observation function. The dynamic mode decomposition provides an approximation of the *Koopman* operator in a finite dimensional space [30].

In previous applications of DMD, the spatial resolution (observation space dimension) of the measured signal is often much greater than the temporal resolution ($m \gg n$). In brain activity measurement, EEG signals have the characteristics of high temporal resolution and low spatial resolution. Therefore, the dimension of the observation space is usually small in the number of time points ($m < n$), which will limit the number of modes and eigenvalues of DMD to the number of EEG channels m , so that the temporal dynamics of the brain cannot be fully displayed. In order to solve the above problems, we used the extended DMD(EDMD) algorithm, combined *Koopman* analysis with the *Takens* time delay embedding theory, and broadened the data matrix by extending the time.

The *Takens* theory shows that the attractor of a dynamic system can be accurately described with historical information [31]. Therefore, time delay embedding can effectively augment the observation function space, that is, use the EEG measurements of the past history to augment the observation function

and generate a new high-dimensional observation vector.

$$\tilde{g}(x_t) = (g(x_t), g(x_{t+\Delta t}), g(x_{t+(s-1)\Delta t})). \quad (3)$$

where Δt is the sampling interval. According to the *Takens* embedding theorem, the original dynamic system is reconstructed. The embedding dimension s needs to satisfy $s \geq 2m + 1$, and m is the original system state dimension.

Therefore, the EEG data in the original sliding window was stacked as a Hankel matrix of $s \times (n - s + 1)$

$$X_{aug} = \begin{bmatrix} x_1 & x_2 & \dots & x_{n-s+1} \\ x_2 & x_3 & \dots & x_{n-s+2} \\ \vdots & \vdots & & \vdots \\ x_{s-1} & x_s & \dots & x_{n-1} \\ x_s & x_{s+1} & \dots & x_n \end{bmatrix}. \quad (4)$$

In practical application, the EDMD method provides a data-driven finite-dimensional approximation for the operator, that is, the operator is approximated by the finite-dimensional matrix.

Assume that the augmented observation matrix satisfies the following discrete linear dynamic description:

$$x_{k+1} = Ax_k. \quad (5)$$

In order to obtain an approximation of matrix A , the m time-delay-augmented EEG measurement data are regarded as the observations of the m system states at the current analysis time. Within snapshots n , the EEG measurement data can be arranged into two $m \times n$ observation data matrices X_{aug}, X'_{aug}

$$X_{aug} = \begin{bmatrix} | & | & & | \\ x_1 & x_2 & \dots & x_n \\ | & | & & | \end{bmatrix} \quad (6)$$

$$X'_{aug} = \begin{bmatrix} | & | & & | \\ x_2 & x_3 & \dots & x_{n+1} \\ | & | & & | \end{bmatrix} \quad (7)$$

where each column of the matrix X' is the state value of each column of the matrix X at the next moment.

Matrix A describes the evolution process of system state X from state X' to state X in the observation space, and its optimal approximation solution is

$$A = X'_{aug} X_{aug}^\dagger. \quad (8)$$

where X^\dagger is the pseudo-inverse of matrix X . In general, matrix X is not a square matrix, so the Moore-Penrose pseudo-inverse needs to be calculated to approximate the inverse of matrix X .

The classical DMD algorithm computes the eigenvalues and eigenvectors of a low-dimensional similarity matrix \tilde{A} by reducing the dimensionality of the observed data to approximate the spectrum of the *Koopman* operator, that is, the main DMD mode [32].

The specific method is to project the data into a low-rank subspace and solve the system matrix \tilde{A} staged in this space. Then, the DMD algorithm uses this low-dimensional operator

\tilde{A} to reconstruct the eigenvectors and eigenvalues of the full-dimensional operator A , thereby extracting the main modes in the system that govern the linear process. The following is the calculation method of the DMD modes:

Perform a truncated singular value decomposition of the matrix with the number of singular values to obtain

$$X \approx U\Sigma V^*. \quad (9)$$

where $*$ denotes the conjugate transpose, extracting its first r singular values and the corresponding singular vectors to form the matrix $U \in \mathbb{C}^{m \times r}, \Sigma \in \mathbb{C}^{r \times r}, V^* \in \mathbb{C}^{r \times n}$. Reduce the rank of the matrix X from n to r . The choice of the parameter r is crucial; too small r or too large r may cause the loss of dynamic information or introduce redundant information, making the modes information inaccurate.

Construct a linear system matrix of system states in low-dimensional space

$$\tilde{A} = U^*AU = U^*X'V\Sigma^{-1}. \quad (10)$$

Compute the eigenvalues and eigenvectors of matrix \tilde{A}

$$\tilde{A}W = W\Lambda. \quad (11)$$

where the matrix Λ is a diagonal matrix; the diagonal elements are the eigenvalues of \tilde{A} , and its corresponding eigenvectors are the column vectors in the matrix W . According to the nature of similar matrices, the eigenvalues of the matrix \tilde{A} are also the eigenvalues of the matrix A . The matrix A corresponding to the eigenvector matrix Φ can be obtained by mapping the eigenvectors W back to the corresponding vectors in the high-dimensional space as follows.

$$\Phi = X'_{aug} V\Sigma^{-1} W. \quad (12)$$

The above DMD method yields a discrete spectrum of the linear system matrix A (approximating *Koopman* operator) in the observation space, where each mode contains eigenvalues and eigenvectors. The eigenvalues describe the frequency and stability of the corresponding frequency components. The eigenvectors describe the spatiotemporal coherent relations, and how to reconstruct the original signal.

The eigenfrequencies of the dynamical system modes can be calculated from the diagonal elements λ of the corresponding eigenvalue matrix Λ as follows.

$$f = \frac{\text{imag}(\ln(\lambda)/\Delta t)}{2\pi}. \quad (13)$$

where Δt is the sampling interval between sample points, and f is the eigenfrequency corresponding to the modes. In this study, the EEG bands of interest were delta (1-4Hz), theta (4-8Hz), alpha (8-13Hz), beta (13-30Hz), and gamma (30-60Hz).

After obtaining the eigenvalues and eigenvectors of the system matrix of the linear system, the original EEG signal can be reconstructed using the modal obtained by DMD.

$$x(t) \approx \sum_{k=1}^r \phi_k e^{\omega_k t} b_k = \Phi e^{\Omega t} b. \quad (14)$$

where r is the number of modes. Φ is the matrix of modes composed by ϕ . Ω is the matrix composed by ω_k . b is the coefficient of each mode.

In the same DMD modes, the EEG components of each channel vibrate according to the corresponding characteristic frequency. Corresponding to different characteristic frequencies, the mode shape may be a real vector or a complex vector. When the mode is a complex mode, the mode shape vector is a complex number, reflecting the phase difference of the EEG signals in each brain region. The oscillational composed of each point form a traveling wave transmitted in space. The amplitude represents the amplitude of each point, and the phase reflects the sequence of vibration occurrences.

D. Sliding window and dynamic functional connectivity

The DMD complex modes reflect the functional connectivity characteristics across channels at the corresponding frequency. This is because in the process of calculating DMD, the multi-channel EEG signals is regarded as a coupled multivariate system. EEG signals can be decomposed into discrete spectrum with corresponding DMD mode shapes, where the DMD modes reflect the spatiotemporal coherent modes of the corresponding rhythm, and also describe the frequency, space and phase information of EEG activity. Their amplitude reflect the amplitude-to-proportion relationship of different channels at a specific frequency, and their phase describe the phase consistency of different channels in EEG, which together describe the functional connectivity characteristics of the whole brain. Sliding window operation for EEG data and applying DMD to the data in each sliding window to extract new mode features can further reflect the changes in brain functional connections over time. Therefore, for whole-brain EEG signals, a series of sliding windows can generate a set of features that contain changes in dynamic functional connections between multiple channels. Since this new feature contains the changes of each channel frequency energy and phase with time, this new mode feature vector contains time, spatial, frequency, and phase changes that reflect dynamic brain connections. In this paper, the ACSP method is used as a spatial filter to extract the variance information of the changes in brain functional connections in each sample as the core information of FOG detection and prediction.

E. Spatial filtering with analytic common spatial pattern method

The ACSP method is a variant of the CSP method. The ACSP method converts the original EEG signal into an analytic signal containing both amplitude and phase information through discrete Hilbert transform. A complex-valued spatial filter is then trained according to the analytic signal and used for spatial filtering of the analytic signal. Compared with the traditional CSP method, the ACSP complex-valued spatial filter can simultaneously extract the amplitude and phase relationship between spatial positions in the data related to potential phenomena, which makes the technology have additional advantages over the CSP algorithm in identifying

phenomena such as traveling waves in phase-shifting patterns [25], [33].

The DMD method described above can extract the amplitude and phase of all channels at the same time, and obtain the dynamic changes of the coupling between multi-channel EEG. Different from the traditional ACSP that needs to be converted into an analytical complex signal through Hilbert transform, the mode eigenvectors obtained by the DMD method are themselves complex number, and the mode eigenvectors themselves contain certain phase information and amplitude information. Therefore, this paper adopts the complex mode shape sequence that changes dynamically with time as the input of the ACSP method. Studies in [12], [34] have shown that the EEG signal of the theta subband is closely related to the motor planning during the occurrence of FOG. Accordingly, we regarded the theta subband as the frequency component of interest, and cut the components of the theta subband from the DMD modal matrix for analysis.

The mode matrix was obtained from the DMD, and q modes corresponding to the theta rhythm components associated with the FOG episodes were selected from the r system modes to obtain the eigenmatrix of the key complex modes vector under each sliding window as follows.

$$\Phi_t = [\phi_{p(1)}, \phi_{p(2)}, \dots, \phi_{p(q)}]. \quad (15)$$

The system DMD feature vectors under p sliding windows were spliced along the time dimension and the feature data matrix containing time, space, amplitude and phase information in the time period was obtained, which was denoted as

$$D = [\Phi_{t(1)}, \Phi_{t(2)}, \dots, \Phi_{t(p)}]. \quad (16)$$

where the feature matrix $D \in \mathbb{C}^{nq \times p}$. In this paper, the detection and prediction tasks of FOG were converted into binary classification tasks of freezing of gait period and normal gait, transitional gait and normal gait, respectively. Without distinction, the data of the two types of classification tasks are recorded as D_1, D_2 .

In the ACSP process, the complex numerical covariance matrix of D can be obtained by the following equation

$$C_i = E[(D_i - E[D_i])(D_i - E[D_i])^*] (i = 1, 2). \quad (17)$$

where $E[\cdot]$ denotes the expectation operator and $(\cdot)^*$ denotes the covariance transpose. The covariance matrices of the original data after segmentation are calculated separately. C_1 is the expectation of the spatial covariance matrix of the first type of sample data, and C_2 denotes the expectation of the spatial covariance matrix of the second type of sample. C_c denotes the sum of the spatial covariance matrices of the two types of data, then there are

$$C_c = C_1 + C_2. \quad (18)$$

since C_1 and C_2 form a pair of Hermitean semidefinite matrices with real-valued elements in the main diagonal and usually complex-valued non-diagonal elements. Therefore, C_c

is a positive definite matrix, and by the eigenvalue decomposition, then can be obtained

$$C_c = L_c \Lambda_c L_c^T. \quad (19)$$

where L_c is the eigenvector matrix, Λ_c denotes the diagonal array of eigenvalues, and the real-valued eigenvalues in the diagonal matrix Λ_c correspond to the eigencolumn vectors of L_c .

The whitening matrix P can be represented as

$$P = \frac{1}{\sqrt{\Lambda_c}} \cdot U_c^T. \quad (20)$$

The projection of the covariance matrix with the whitening matrix is given by

$$S_1 = P C_1 P^T, S_2 = P C_2 P^T. \quad (21)$$

S_1, S_2 have the same eigenvectors and the sum of the diagonal arrays corresponding to the eigenvalues is a unit array, i.e., the sum of the corresponding eigenvalues is 1, satisfying the following conditions

$$S_1 = B \Lambda_1 B^T, S_2 = B \Lambda_2 B^T. \quad (22)$$

$$\Lambda_1 + \Lambda_2 = I. \quad (23)$$

The projection matrix W_A maximizes the variance of one class of data and minimizes the variance of another class of data, so the classification of two classes of problems can be achieved using the matrix B . Note that, unlike the traditional CSP method, the projection matrix W_{ACSP} here is a complex-valued projection matrix.

$$W_A = B^T P. \quad (24)$$

The optimal feature space was obtained by projecting the feature matrix.

$$Z_1 = W_A D_1, Z_2 = W_A D_2. \quad (25)$$

According to a certain type of characteristic value, the feature information with the best distinguishing characteristics is mainly concentrated in the head and tail of the feature matrix. Therefore, the data of the first m rows and the last m rows ($2m \leq M$) are selected as the feature matrix for ACSP feature extraction.

In the dimensionality-reduced feature space, the logarithm of variance F_1, F_2 were extracted as the final classification feature, where F_i was the normalized feature matrix of the i th sample.

$$F_i = \ln\left(\frac{\text{var}(Z_i)}{\sum_{n=1}^{2m} \text{var}(Z_i)}\right). \quad (26)$$

From the ACSP method, a representation method $A_W = W_A^{-1}$ of a set of spatial patterns of dynamic brain functional connections can be obtained. The column vectors of A_W represented the spatial component associated with each diagonal element in Λ_1 and Λ_2 . Compared with traditional

CSP algorithms, spatial filters and spatial patterns can only represent the spatial transition or reverse change by whether the coefficient value is positive or negative. The spatial filter and spatial pattern of ACSP consist of complex valued elements. These elements can be divided into a magnitude and a phase component, which can better distinguish and represent underlying brain activity.

F. Classifiers for FOG detection and prediction

In the FOG detection task, we used a simple linear discriminant analysis (LDA) method to highlight the validity of the proposed features. LDA is a binary linear classifier commonly used in EEG recognition problems. By finding an optimal projection direction in the projection space, the intra-class variance between similar samples is minimized and the inter-class variance between different classes of samples is maximized [35]. The dimensionality-reduced features normalized by DMD-ACSP were put into the LDA classifier for training to obtain the FOG classifier model.

In the FOG prediction task, we considered that there was less data in the transitional gait period, resulting in a high degree of imbalance in the classification task, that is, the number of samples in the normal gait period was much higher than that in the transitional gait period. To solve the above problems, the impact of unbalanced data was improved by changing the data sampling and selecting a boosting classifier. To this end, we adopted the RUSBoost algorithm, which is a method that combines random undersampling with the Adaboost algorithm [36]. Random undersampling consists of randomly extracting a certain amount of majority class samples and minority classes from the dataset to form a balanced training dataset. Before training the weak classifier, the RUS method is used to extract the training dataset for weak classifier training. The Adaboost algorithm trains and iterates on the weak classifier, adjusts the weights after many iterations, and finally obtains a improved strong classifier. The data imbalance of the FOG prediction task made the RUSBoost algorithm an ideal classification algorithm.

G. Transfer learning(TL)

The DMD-ACSP method extracted the phase information and amplitude information in the spatiotemporal coherent modes of EEG at corresponding frequencies, and considered the explicit amplitude and phase differences between different spatial locations. Although the extracted feature patterns had good interpretability and intra-individual classification performance, the data distribution varied for each new subject due to the large individual differences in EEG and the inherent non-stationarity of the EEG signal. This resulted in much lower accuracy for cross-individual classification tasks.

To address the problem of low accuracy in cross-individual classification tasks, we considered transfer learning (TL), which uses data from the source domain (existing subjects) to aid in the calibration of the target domain (new subjects). In this paper, we referred to the EEG migration learning approach provided by [37] to change the data distribution and adjust the spatial filtering and classifier components by the TL method.

Due to individual differences, EEG of different subjects usually showed different marginal probability distributions. Therefore, we adopted Euclidean alignment to initially align the EEG data of the target domain with the data of the source domain.

For Euclidean alignment of the source domain, the first step was calculated as follows.

$$\bar{R}_s = \frac{1}{N_s} \sum_{n=1}^{N_s} X_s^n (X_s^n)^T. \quad (27)$$

where X_s^n is the data of the n th EEG experiment in the source domain and N_s is the number of EEG experiments in the source domain. This equation calculated the covariance matrix of all source domains and finds the corresponding Euclidean arithmetic mean. Then the alignment operation was performed.

$$\tilde{X}_s^n = \bar{R}_s^{-\frac{1}{2}} X_s^n. \quad (28)$$

For the target subjects, the same Euclidean alignment could be performed. This allowed the spatial covariance matrix of different subjects to be transformed into the form of a unit matrix, allowing for a more consistent distribution of EEG trials.

In cross-domain recognition, the spatial filter W computed with the target subject's data only may not be reliable due to the small sample data of the target subject. We referred to the combined CSP method to train the spatial filter W by mixing the source domain samples with the target domain samples. All samples from both domains were treated equally.

Again, when the target domain samples were too small, the classifier may have poorer classification results. The combined classifier was a worthwhile TL method that joined labelled samples from the source and target domains to train the corresponding classifier. Here, all samples were set to the same weights.

H. Baseline models and performance evaluation

To investigate the effectiveness of the proposed DMD-ACSP extracted features, we compared it with several competing FOG feature extraction methods. According to the existing literature on using EEG detection and prediction of FOG, the Short-Time Fourier Transform (STFT) and Wavelet Transform (WT) were selected as baseline feature extraction methods for comparative analysis.

STFT is a simple time-frequency domain analysis method. By performing a fast Fourier transform on the data in the sliding window, each power spectrum was represented as a percentage of the total power in the 0.5-60 Hz frequency window to normalize, thereby extracting the power spectral density (PSD).

The wavelet transform is an ideal tool for time-frequency analysis and processing of non-stationary signals. It inherits and develops the idea of short-time Fourier transform, while overcoming the drawback of window size not varying with frequency, and can provide a "time-frequency" window that varies with frequency. In wavelet transform time-frequency

feature extraction, wavelet energy (WE) represents the energy distribution in the frequency domain. In the current EEG-based FOG detection method, the WE feature has showed good classification performance and is the mainstream classification feature extraction method.

To demonstrate the contributions of DMD and ACSP in the proposed DMD-ACSP method, we investigated the contributions of DMD and ACSP algorithms to classification performance using ablation experiments, respectively. In order to ensure the fairness of the comparison, we used the same preprocessing method, window size and classifier for all feature extraction methods.

We evaluated the effectiveness of the DMD-ACSP model in FOG feature extraction studies through two tasks. The first task was to detect interindividual FOG episodes. In this task, we classified data from freezing of gait periods versus normal gait periods for each of ten subjects. The second task was to predict cross-individual FOG episodes. We classified the data for the transition gait periods versus the normal gait periods for the subjects separately. We used the leave-one-out cross-validation (LOOCV) method. In each fold, data from nine subjects were used to train the DMD-ACSP model, and the features of the remaining subjects were generated by these models. The performance of this model was then tested using the following criteria: accuracy and sensitivity

$$\text{Accuracy} = (TP + TN) / (TP + TN + FP + FN). \quad (29)$$

$$\text{Sensitivity} = TP / (TP + FN). \quad (30)$$

where TP, TN, FP, and FN are samples of the number of true positives, true negatives, false positives, and false negatives, respectively.

III. RESULTS

A. DMD power spectrum

Take the record in Sub.1 of the EEG dataset of FOG as an example and apply DMD to it. After the EEG was decomposed, each DMD mode corresponded to a characteristic frequency. At the same characteristic frequency, the mode energy of the DMD can be calculated as $P = |\Phi|^2$. Figure 2 showed the power spectrum distribution of the DMD modes at different frequencies and a comparison of the power spectrum calculated by the Fast Fourier Transform (FFT). The DMD power spectrum has many similarities with the FFT power spectrum. For example, when the frequency is 5Hz, the power reaches the highest value, and as the frequency increases, the power of both gradually decays, which shows that the DMD modes can accurately reflect the time-frequency characteristics of EEG. In addition, the DMD modes are calculated based on the EEG data of all channels, so that its spectrum is sparse, which reveals the key spatiotemporal coherent modes of brain activity. The FFT obtains the energy of the corresponding frequency by calculating the EEG data of each channel separately. Compared with FFT, the DMD power spectrum reflects the energy of each mode, which represents the characteristics of whole-brain functional connectivity at specific frequencies, not just the energy of EEG signals.

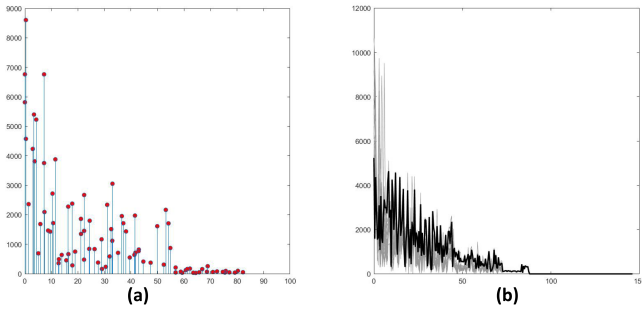


Fig. 2. (a) DMD power spectrum. (b) FFT power spectrum (grey lines show all 25 channels, bold black lines show average).

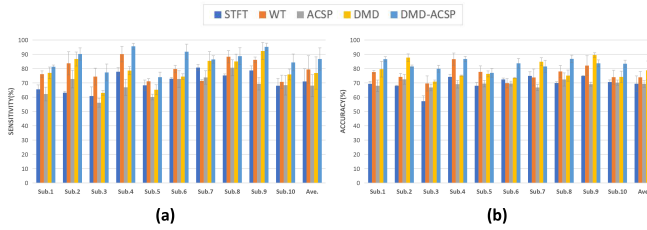


Fig. 3. The averaged (a) sensitivity and (b) accuracy for each combination of features for ten subjects under the detection task. Ave. is the average metric for ten subjects.

B. Comparative study on metrics of FOG detection

Figure 3 shows the ability of DMD-ACSP and other methods to extract features to detect FOG. It can be found that all indicators of DMD-ACSP method have higher performance than STFT method. Among them, the sensitivity of DMD-ACSP method is $12.5 \pm 4.8\%$ higher than that of STFT, and the increment of accuracy is $13.8 \pm 3.4\%$. This comparison shows that the features extracted by our method are more effective in FOG detection than simple time-frequency domain features. At the same time, compared with WT, the DMD-ACSP method improves the sensitivity by $7.4 \pm 2.1\%$ and the accuracy by $5.5 \pm 1.8\%$. Consistent performance improvements were shown in each subject's metrics. These results showed that the DMD-ACSP method can effectively improve the FOG detection performance compared with the time-frequency analysis method.

TABLE I

AVERAGED METRICS OF FIVE FEATURE EXTRACTION METHODS UNDER FOG DETECTION TASK

Metric	STFT	WT	ACSP	DMD	DMD-ACSP
Sensitivity(%)	71.0 ± 2.9	76.1 ± 5.7	61.2 ± 5.7	74.2 ± 2.6	83.5 ± 4.3
Accuracy(%)	75.3 ± 3.5	83.6 ± 2.4	68.6 ± 4.2	76.4 ± 2.7	89.1 ± 3.6

In order to further study the contribution of DMD method and ACSP method in FOG classification, we carried out ablation experiments. The Hilbert transform was used to train the ACSP model in the dataset, and the corresponding spatial features were extracted. It can be observed that if the features extracted by the ACSP model are simply used for the classification of the detection task, the effect is not satisfactory. Compared with time-frequency methods such as WT and STFT, the performance of ACSP is significantly

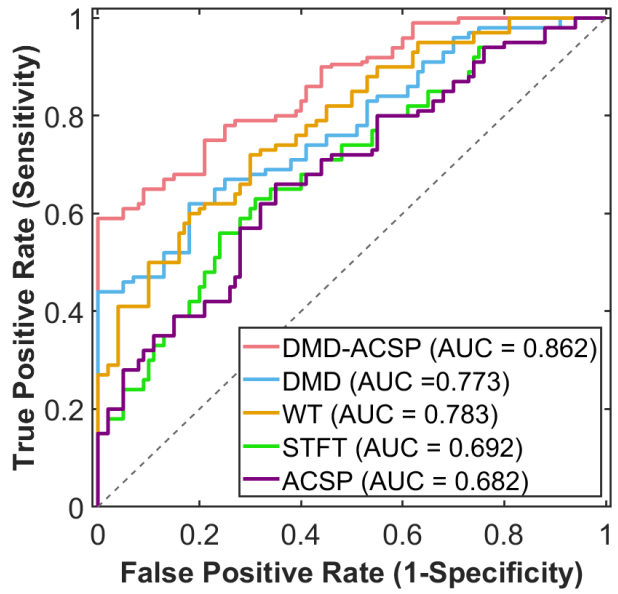


Fig. 4. Receiver Operating Characteristic (ROC) curves in the binary classification performed in the FOG detection task. The inset shows the area under curve (AUC).

lower than that of both. However, when using the DMD-ACSP method and combining the time-frequency method with the spatial filtering algorithm, the best performance can be obtained. DMD-ACSP was much better than ACSP, the average sensitivity of the subjects was increased by $22.3 \pm 1.6\%$, and the accuracy was improved by $20.5 \pm 2.2\%$. On the other hand, only the DMD method was used to extract time-frequency features, and the effect was also not optimal. The DMD-ACSP method also outperformed DMD, and the average sensitivity and accuracy of the subjects were improved by $9.3 \pm 4.8\%$ and $12.7 \pm 5.4\%$, respectively. This showed that after DMD-ACSP utilized time-frequency features and spatial features, its performance in detecting FOG has been significantly improved. In Figure 4, the receiver operating characteristic (ROC) curve further illustrates the effectiveness of the proposed method. It can be observed that the DMD-ACSP method outperforms other methods in classification performance at all thresholds.

C. Comparative study on FOG prediction

Similar to above, we evaluated the classification performance of the five models under the FOG prediction task. As shown in Figure 5 and Table 2, the DMD-ACSP method still exhibited a fairly good performance. The features extracted by the DMD-ACSP method were still quite competitive compared to the time-frequency features. Compared with the baseline STFT method, the DMD-ACSP method had an average sensitivity improvement of $15.7 \pm 6.5\%$ and an accuracy improvement of $14.1 \pm 5.4\%$ for subjects. Compared with the WT method, the average sensitivity and accuracy of DMD-ACSP were $7.3 \pm 4.3\%$ and $9.6 \pm 6.1\%$ higher than those of the WT method, and the classification performance was significantly improved.

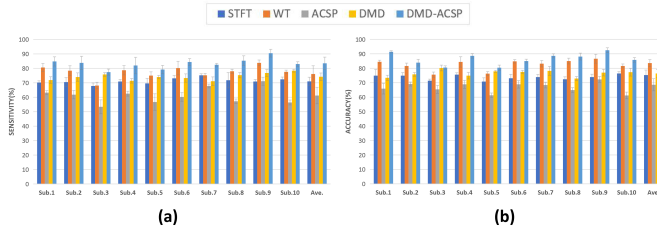


Fig. 5. The averaged (a) sensitivity and (b) accuracy for each combination of features for ten subjects under the prediction task. Ave. is the average metric for ten subjects.

TABLE II

AVERAGED METRICS OF FIVE FEATURE EXTRACTION METHODS UNDER FOG PREDICTION TASK

Metric	STFT	WT	ACSP	DMD	DMD-ACSP
Sensitivity(%)	71.0±8.9	79.4±9.6	68.1±7.7	76.9±11.3	86.7±7.8
Accuracy(%)	69.4±5.5	73.9±4.1	69.3±2.3	78.8±6.5	83.5±3.2

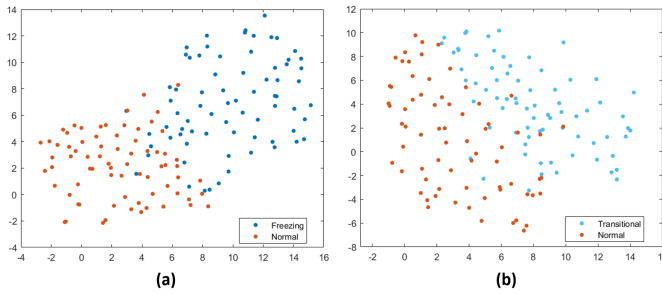


Fig. 6. Visualization of DMD-ACSP features of different phases by t-SNE method. (a) is the detection task, (b) is the prediction task.

The task of the DMD-ACSP method was to extract the dynamic functional connections of the EEG, then separated the DMD patterns with spatiotemporal coherent modes, and finally extracted the spatial patterns with significant dynamic functional connection changes through complex-valued spatial filtering. In order to verify the separability of the DMD-ACSP features, Figures 6(a) and (b) show the representation of DMD-ACSP features in a two-dimensional feature space for normal gait period versus freezing of gait period, and normal gait period versus transitional gait period, respectively. It can be seen from the figure that each type of gait is divided into different clusters with clear classification boundaries. The type of gait is well characterized using the DMD-ACSP features.

D. Spatial patterns in the dynamic functional connectivity of three different gaits

This section further analyses the spatial activation mode characterization of dynamic functional connections of different gaits extracted by DMD-ACSP. Figure 7 shows the most dominant spatial pattern A_W (defined in Section 2.4) of the three gaits extracted by DMD-ACSP after spatial filtering. Figures 7 (a) and (b) show the spatial pattern of the largest difference between freezing of gait versus normal gait, and the spatial pattern of the largest difference between transitional gait versus normal gait, respectively.

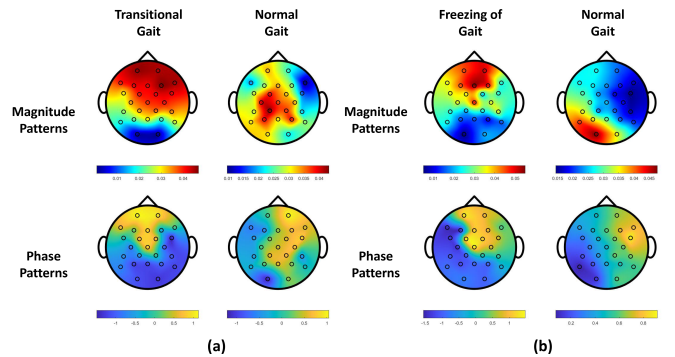


Fig. 7. Major spatial features for gait classification on the dataset by the DMD-ACSP method. In (a) shows that the frontal as well as parietal parts of the brain in transitional gait exhibit a strong pattern of amplitude activation, while phase coupling is also shown in the prefrontal and parietal parts. In (b) it is shown that the prefrontal and parietal regions of the brain in the FOG exhibit similar patterns of amplitude and phase activation.

We can observe that in the prediction task, the frontal and parietal lobes of the transitional gait show strong amplitude activation patterns, and the prefrontal and parietal lobes also show strong phase coupling. In the DMD-ACSP model, this is interpreted as a more active dynamic functional connection change between the prefrontal and parietal lobes during the transitional gait period. The frontal region is mainly responsible for the brain's motor preparation and cognitive decision-making functions, and the activation of the parietal region may be related to motor functions such as dystonia. This may mean that the freezing sensation of FOG is not affected by only one brain region, but is the result of the combined influence of multiple brain regions. Compared with the transitional gait in the early stage of freezing, the main active areas of normal gait are concentrated in the motor function area.

In the detection task, the prefrontal and parietal regions of the brain in FOG show similar amplitude and phase activation patterns, indicating a certain phase-amplitude coupling between the prefrontal and parietal lobes. Compared with freezing of gait, the main active areas of normal gait are concentrated in the occipital visual area.

Studies have shown that [38], in the middle and late stages of Parkinson's disease, the originally independent nucleus discharges are extremely synchronized, indicating that the changes in the dynamic functional connection relationship between different brain regions are related to the occurrence of FOG, which is related to our proposed. The characteristics of the dynamic functional connection patterns are consistent.

IV. DISCUSSIONS

Since the EEG signal reflects the electrophysiological changes during the occurrence of FOG, EEG based methods may be able to predict the occurrence of movement disorders more accurately than gait information, such as accelerations and angular velocities. In this study, a new EEG pattern recognition technology has been proposed to study the role of EEG in the detection and prediction of FOG where the DMD-ACSP method was used to extract dynamic connection

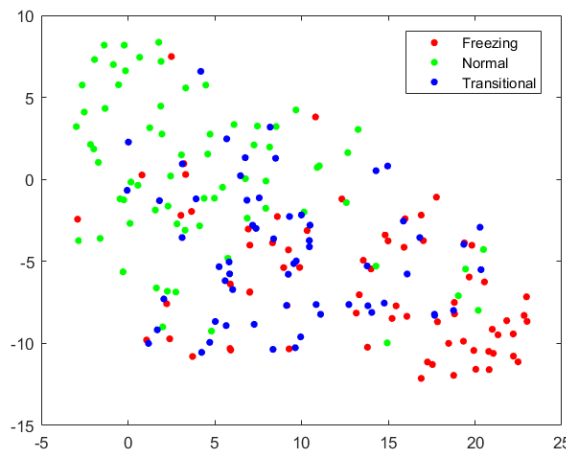


Fig. 8. Visualization of DMD features for normal gait, transition gait and FOG by t-SNE method.

pattern changes in the brain dynamic system. Experimental results showed that the method achieves the most encouraging performance in the FOG classification task compared with traditional feature extraction methods.

Common used EEG feature extraction methods for detecting or predicting FOG include Fourier transform, wavelet transform, phase synchronization analysis and directional transfer function and independent component analysis, and so on. In the study [13], 86.0% sensitivity and 80.2% accuracy of FOG prediction were achieved by STFT and WT. In the study [17], 85.86% sensitivity and 80.25% specificity of FOG prediction were obtained by using directional transfer function and independent component analysis. In the detection task, study [14] obtained about 75% of the sensitivity and accuracy of FOG detection by extracting power spectral density, centroid frequency and power spectral entropy. [15] Using S-transform to achieve 84.2% sensitivity and 88.0% specificity of FOG detection during turns. Compared with previous research results, the DMD-ACSP method achieves leading performance in EEG-based FOG detection and prediction.

Properly selected features should be of good interpretability and can well characterize the transition from normal gaits to freezing of gaits. In Figure 8, the DMD modes of normal gait, transitional gait and FOG were dimensionally reduced by t-SNE method and visualized. The patterns clearly show the transition from normal gaits to FOG in the feature space, where most transition gaits locate between the normal and freezing gait, although they are not well separated because no ACSP were applied. This indicates that the spatiotemporal coherent modes are closely related to the occurrence of FOG.

Compared with the existing EEG-based FOG recognition methods, the DMD-ACSP method has several obvious advantages. First, the proposed DMD model extracts EEG modes features based on the dynamic interaction relationships between EEG channels. Therefore, the DMD-ACSP method can extract good mode features, i.e., spatiotemporal coherent modes, in a finer time scale. These mode features can show more stable classification performance in cross-

individual tasks. Since time-frequency analysis methods such as STFT, WT, and HHT tended to extract features based on individual channels, they usually failed to reflect the interactions between different channels in the EEG signal, making the time-frequency spectrum estimation vulnerable to noise interference, which affected decoding accuracy and generalization performance [39], [40]. Second, for each EEG modes characterizing spatiotemporal correlation information, its corresponding spatiotemporal coherent modes reflect the functional connectivity relationships between different regions of the brain at that rhythm, i.e., it includes the relative intensity of brain activity (amplitude information) and also the temporal differences in brain activity between regions (phase information). Several recent studies have shown that functional connectivity relationships characterized by phase amplitude coupling are a promising approach to study cognitive processes [41], [42]. In contrast, STFT, WT and most existing time-frequency methods did not utilize phase information as a classification feature, which left the information of phase coupling underutilized. Third, based on Koopman operator theory, the DMD method treats the EEG signal as a high-dimensional observed variable of brain activity, and the obtained modes characterize the nonlinear dynamical behaviour of the brain from a linear observation space. In contrast, previous time-frequency methods usually ignored the non-smooth and non-linear nature of EEG and fit the non-linear EEG signal with a linear transformation. This resulted in the loss of a part of dynamic information [43]. Therefore, DMD-ACSP can improve the classification performance of detecting and predicting FOG.

In addition, the DMD method provides a new linear brain dynamic decoding and control method. Compared with the traditional method of functional connection between two channels, the DMD mode provides a spatiotemporal coherent mode matrix, which can represent the dynamic functional connections of the whole brain region. This also makes the DMD method have the potential to dynamically measure and decode the functional network of the brain. At the same time, based on the Koopman operator spectrum theory, the DMD method reveals the change law of EEG in the measurement space, which promises to provide a new theoretical basis and control model for the neural regulation of FOG in the brain network [44].

However, there are still some limitations in our study. First, because whole brain EEG channels were used in our method, the demand for EEG measurement devices is higher than methods based on small number of EEG channels and the computational cost can be large. This is may limited the application of the DMD-ACSP method in daily life applications. Second, the number of subjects in this study was small, and the data of some patients were heavily unbalanced, which may worsen the generalization ability of the results. Therefore, it is worthy to further evaluate the proposed method on a larger population to obtain more general conclusions.

V. CONCLUSION

A new FOG detection and prediction method which focuses on the dynamic functional connectivity of whole brain regions

has been proposed. Using the DMD algorithm, spatiotemporal coherent modes of FOG are extracted from EEG data which represent the functional connectivity of the whole brain. Applying sliding windows, an ACSP based spatially filtered is used to extract the amplitude and phase fluctuation of the spatiotemporal modes during FOG. Experimental results have showed that the DMD-ACSP method produces excellent detection and prediction of FOG. The dynamic spatiotemporal coherent modes not only revealed the different spatial patterns among normal, pre-freezing and freezing of gait but also characterizes the transition of the brain states from normal gaits to freezing gaits in the feature space. This may provide new insight into the mechanism of freezing of gait and shed light on accurate neuromodulation.

ACKNOWLEDGMENT

Author Guo Yuzhu thanked the Beijing Natural Science Foundation Project (Project No.4202040) and the Natural Science Foundation Project (Project No.61876015) for their financial support for this research.

REFERENCES

- [1] W. Poewe, K. Seppi, C. M. Tanner, G. M. Halliday, P. Brundin, J. Volkmann, A.-E. Schrag, and A. E. Lang, "Parkinson disease," *Nature Reviews Disease Primers*, vol. 3, p. 17013, Dec. 2017.
- [2] J. G. Nutt, B. R. Bloem, N. Giladi, M. Hallett, F. B. Horak, and A. Nieuwboer, "Freezing of gait: moving forward on a mysterious clinical phenomenon," *The Lancet Neurology*, vol. 10, pp. 734–744, Aug. 2011.
- [3] M. Mancini, B. R. Bloem, F. B. Horak, S. J. Lewis, A. Nieuwboer, and J. Nonnkes, "Clinical and methodological challenges for assessing freezing of gait: Future perspectives," *Movement Disorders*, vol. 34, pp. 783–790, June 2019.
- [4] D. Weiss, A. Schoellmann, M. D. Fox, N. I. Bohnen, S. A. Factor, A. Nieuwboer, M. Hallett, and S. J. G. Lewis, "Freezing of gait: understanding the complexity of an enigmatic phenomenon," *Brain*, vol. 143, pp. 14–30, Jan. 2020.
- [5] C. C. Walton, J. M. Shine, J. M. Hall, C. O'Callaghan, L. Mowszowski, M. Gilat, J. Y. Y. Szeto, S. L. Naismith, and S. J. G. Lewis, "The major impact of freezing of gait on quality of life in Parkinson's disease," *Journal of Neurology*, vol. 262, pp. 108–115, Jan. 2015.
- [6] Y. Guo, D. Huang, W. Zhang, L. Wang, Y. Li, G. Olmo, Q. Wang, F. Meng, and P. Chan, "High-accuracy wearable detection of freezing of gait in Parkinson's disease based on pseudo-multimodal features," *Computers in Biology and Medicine*, vol. 146, p. 105629, July 2022.
- [7] Y. Guo, L. Wang, Y. Li, L. Guo, and F. Meng, "The Detection of Freezing of Gait in Parkinson's Disease Using Asymmetric Basis Function TV-ARMA Time-Frequency Spectral Estimation Method," *IEEE Transactions on Neural Systems and Rehabilitation Engineering*, vol. 27, pp. 2077–2086, Oct. 2019.
- [8] L. Mesin, P. Porcu, D. Russu, G. Farina, L. Borzì, W. Zhang, Y. Guo, and G. Olmo, "A Multi-Modal Analysis of the Freezing of Gait Phenomenon in Parkinson's Disease," *Sensors*, vol. 22, p. 2613, Mar. 2022.
- [9] M. Günther, R. P. Bartsch, Y. Miron-Shahar, S. Hassin-Baer, R. Inzelberg, J. Kurths, M. Plotnik, and J. W. Kantelhardt, "Coupling Between Leg Muscle Activation and EEG During Normal Walking, Intentional Stops, and Freezing of Gait in Parkinson's Disease," *Frontiers in Physiology*, vol. 10, p. 870, July 2019.
- [10] S. Mazilu, A. Calatroni, E. Gazit, A. Mirelman, J. M. Hausdorff, and G. Troster, "Prediction of Freezing of Gait in Parkinson's From Physiological Wearables: An Exploratory Study," *IEEE Journal of Biomedical and Health Informatics*, vol. 19, pp. 1843–1854, Nov. 2015.
- [11] Y. Wei, B. Zhu, C. Hou, C. Zhang, and Y. Sui, "Interactive Video Acquisition and Learning System for Motor Assessment of Parkinson's Disease," in *Proceedings of the Thirtieth International Joint Conference on Artificial Intelligence*, (Montreal, Canada), pp. 5024–5027, International Joint Conferences on Artificial Intelligence Organization, Aug. 2021.
- [12] V. J. Geraedts, L. I. Boon, J. Marinus, A. A. Gouw, J. J. van Hilten, C. J. Stam, M. R. Tannemaat, and M. F. Contarino, "Clinical correlates of quantitative EEG in Parkinson disease: A systematic review," *Neurology*, vol. 91, pp. 871–883, Nov. 2018.
- [13] A. M. A. Handojoseno, J. M. Shine, T. N. Nguyen, Y. Tran, S. J. G. Lewis, and H. T. Nguyen, "The detection of Freezing of Gait in Parkinson's disease patients using EEG signals based on Wavelet decomposition," p. 4.
- [14] A. M. A. Handojoseno, J. M. Shine, T. N. Nguyen, Y. Tran, S. J. G. Lewis, and H. T. Nguyen, "Analysis and Prediction of the Freezing of Gait Using EEG Brain Dynamics," *IEEE Transactions on Neural Systems and Rehabilitation Engineering*, vol. 23, pp. 887–896, Sept. 2015.
- [15] Q. T. Ly, A. A. Handojoseno, M. Gilat, R. Chai, K. A. Ehgoetz Martens, M. Georgiades, G. R. Naik, Y. Tran, S. J. Lewis, and H. T. Nguyen, "Detection of turning freeze in Parkinson's disease based on S-transform decomposition of EEG signals," in *2017 39th Annual International Conference of the IEEE Engineering in Medicine and Biology Society (EMBC)*, (Seogwipo), pp. 3044–3047, IEEE, July 2017.
- [16] Q. T. Ly, A. A. Handojoseno, M. Gilat, N. Nguyen, R. Chai, Y. Tran, S. J. G. Lewis, and H. T. Nguyen, "Detection of Gait Initiation Failure in Parkinson's disease patients using EEG signals," in *2016 38th Annual International Conference of the IEEE Engineering in Medicine and Biology Society (EMBC)*, (Orlando, FL, USA), pp. 1599–1602, IEEE, Aug. 2016.
- [17] A. M. A. Handojoseno, J. M. Shine, M. Gilat, T. N. Nguyen, Y. Tran, S. J. Lewis, and H. T. Nguyen, "Prediction of freezing of gait using analysis of brain effective connectivity."
- [18] F. Riaz, A. Hassan, S. Rehman, I. K. Niazi, and K. Dremstrup, "EMD-Based Temporal and Spectral Features for the Classification of EEG Signals Using Supervised Learning," *IEEE Transactions on Neural Systems and Rehabilitation Engineering*, vol. 24, pp. 28–35, Jan. 2016.
- [19] K. Fu, J. Qu, Y. Chai, and Y. Dong, "Classification of seizure based on the time-frequency image of EEG signals using HHT and SVM," *Biomedical Signal Processing and Control*, vol. 13, pp. 15–22, Sept. 2014.
- [20] P. J. Schmid, "Dynamic mode decomposition of numerical and experimental data," *Journal of Fluid Mechanics*, vol. 656, pp. 5–28, Aug. 2010.
- [21] P. J. Schmid, "Dynamic Mode Decomposition and Its Variants," *Annual Review of Fluid Mechanics*, vol. 54, pp. 225–254, Jan. 2022.
- [22] B. W. Brunton, L. A. Johnson, J. G. Ojemann, and J. N. Kutz, "Extracting spatial-temporal coherent patterns in large-scale neural recordings using dynamic mode decomposition," *Journal of Neuroscience Methods*, vol. 258, pp. 1–15, Jan. 2016.
- [23] M. S. J. Solaija, S. Saleem, K. Khurshid, S. A. Hassan, and A. M. Kamboh, "Dynamic Mode Decomposition Based Epileptic Seizure Detection from Scalp EEG," *IEEE Access*, vol. 6, pp. 38683–38692, 2018.
- [24] H. Ramoser, J. Muller-Gerking, and G. Pfurtscheller, "Optimal spatial filtering of single trial EEG during imagined hand movement," *IEEE Transactions on Rehabilitation Engineering*, vol. 8, pp. 441–446, Dec. 2000.
- [25] O. Falzon, K. P. Camilleri, and J. Muscat, "The analytic common spatial patterns method for EEG-based BCI data," *Journal of Neural Engineering*, vol. 9, p. 045009, Aug. 2012.
- [26] W. Zhang, Z. Yang, and H. Li, "Multimodal Dataset of Freezing of Gait in Parkinson's Disease," <https://doi.org/10.1038/s41597-022-01713-8>, Sci Data 9, 606 (2022).
- [27] N. Kannathal, U. R. Acharya, C. Lim, and P. Sadasivan, "Characterization of EEG—A comparative study," *Computer Methods and Programs in Biomedicine*, vol. 80, pp. 17–23, Oct. 2005.
- [28] J. Kaur and A. Kaur, "A review on analysis of EEG signals," in *2015 International Conference on Advances in Computer Engineering and Applications*, (Ghaziabad, India), pp. 957–960, IEEE, Mar. 2015.
- [29] B. O. Koopman, "Hamiltonian Systems and Transformation in Hilbert Space," *Proceedings of the National Academy of Sciences*, vol. 17, pp. 315–318, May 1931.
- [30] M. O. Williams, I. G. Kevrekidis, and C. W. Rowley, "A Data-Driven Approximation of the Koopman Operator: Extending Dynamic Mode Decomposition," *Journal of Nonlinear Science*, vol. 25, pp. 1307–1346, Dec. 2015.
- [31] J. C. Robinson, "A topological delay embedding theorem for infinite-dimensional dynamical systems," *Nonlinearity*, vol. 18, pp. 2135–2143, Sept. 2005.
- [32] S. L. Brunton, B. W. Brunton, J. L. Proctor, and J. N. Kutz, "Koopman Invariant Subspaces and Finite Linear Representations of Nonlinear

- Dynamical Systems for Control," *PLOS ONE*, vol. 11, p. e0150171, Feb. 2016.
- [33] L. F. Nicolas-Alonso, R. Corralejo, D. Alvarez, and R. Hornero, "Analytic common spatial pattern and adaptive classification for multiclass motor imagery-based BCI," in *2013 6th International IEEE/EMBS Conference on Neural Engineering (NER)*, (San Diego, CA, USA), pp. 1084–1087, IEEE, Nov. 2013.
- [34] J. Shine, A. Handojoseno, T. Nguyen, Y. Tran, S. Naismith, H. Nguyen, and S. Lewis, "Abnormal patterns of theta frequency oscillations during the temporal evolution of freezing of gait in Parkinson's disease," *Clinical Neurophysiology*, vol. 125, pp. 569–576, Mar. 2014.
- [35] A. Tharwat, T. Gaber, A. Ibrahim, and A. E. Hassanien, "Linear discriminant analysis: A detailed tutorial," *AI Communications*, vol. 30, pp. 169–190, May 2017.
- [36] C. Seiffert, T. M. Khoshgoftaar, J. Van Hulse, and A. Napolitano, "RUSBoost: A Hybrid Approach to Alleviating Class Imbalance," *IEEE Transactions on Systems, Man, and Cybernetics - Part A: Systems and Humans*, vol. 40, pp. 185–197, Jan. 2010.
- [37] D. Wu, X. Jiang, and R. Peng, "Transfer learning for motor imagery based brain-computer interfaces: A tutorial," *Neural Networks*, vol. 153, pp. 235–253, Sept. 2022.
- [38] R. Mehanna, S. Moore, J. G. Hou, A. I. Sarwar, and E. C. Lai, "Comparing clinical features of young onset, middle onset and late onset Parkinson's disease," *Parkinsonism & Related Disorders*, vol. 20, pp. 530–534, May 2014.
- [39] V. K. Harpale and V. K. Bairagi, "Time and frequency domain analysis of EEG signals for seizure detection: A review," in *2016 International Conference on Microelectronics, Computing and Communications (MicroCom)*, (Durgapur, India), pp. 1–6, IEEE, Jan. 2016.
- [40] S. Vaid, P. Singh, and C. Kaur, "EEG Signal Analysis for BCI Interface: A Review," in *2015 Fifth International Conference on Advanced Computing & Communication Technologies*, (Haryana, India), pp. 143–147, IEEE, Feb. 2015.
- [41] V. Grigorovsky, D. Jacobs, V. L. Breton, U. Tufa, C. Lucasius, J. M. del Campo, Y. Chinvarun, P. L. Carlen, R. Wennberg, and B. L. Bardakjian, "Delta-gamma phase-amplitude coupling as a biomarker of postictal generalized EEG suppression," *Brain Communications*, vol. 2, p. fcaa182, July 2020.
- [42] R. Gong, M. Wegscheider, C. Mühlberg, R. Gast, C. Fricke, J.-J. Rumpf, V. V. Nikulin, T. R. Knösche, and J. Classen, "Spatiotemporal features of beta-gamma phase-amplitude coupling in Parkinson's disease derived from scalp EEG," *Brain*, vol. 144, pp. 487–503, Mar. 2021.
- [43] C. Stam, "Nonlinear dynamical analysis of EEG and MEG: Review of an emerging field," *Clinical Neurophysiology*, vol. 116, pp. 2266–2301, Oct. 2005.
- [44] Y.-J. Xie, Q. Gao, C.-Q. He, and R. Bian, "Effect of repetitive transcranial magnetic stimulation on gait and freezing of gait in parkinson disease: A systematic review and meta-analysis," *Archives of Physical Medicine and Rehabilitation*, vol. 101, no. 1, pp. 130–140, 2020.